ISSN 1070-3284, Russian Journal of Coordination Chemistry, 2016, Vol. 42, No. 3, pp. 207–216. © Pleiades Publishing, Ltd., 2016.

Synthesis and Structural Determination of Mononuclear Eight-Coordinate (EnH)[Lu^{III}(Egta)] · $2H_2O$ and 2D Ladder-Like Nine-Coordinate (EnH_2)[Y^{III}(Egta)(H_2O)]$_2$ · $6H_2O$[1]

B. Li, C. Qin, D. Y. Kong, and J. Wang*

Department of Chemistry, Liaoning University, Shenyang, 110036 P.R. China

**e-mail: wangjuncomplex890@126.com*

Received April 4, 2015

Abstract—Two novel lanthanide complexes, (EnH)[Lu^{III}(Egta)] · $2H_2O$ (**I**) and (EnH_2)[Y^{III}(Egta)H_2O]$_2$ · $6H_2O$ (**II**), where En = ethylenediamine and H_4Egta = ethyleneglycol-bis-(2-aminoethylether)-*N*,*N*,*N*′,*N*′-tetraacetic acid, have been successfully synthesized through direct heating reflux and their molecular crystal structures were determined by FT-IR spectroscopy, thermal analysis and single crystal X-ray diffraction techniques (CIF files CCDC nos. 966211 (**I**) and 966210 (**II**)). X-ray diffraction reveals that **I** has a eight-coordinate mononuclear structure with distorted square antiprismatic conformation. The reason that the Lu(III) adopts a eight-coordinate conformation is the small ionic radius and more *f*-orbital electrons, which generates a relatively small coordination number. Complex **I** crystallizes in a orthorhombic system with $Pca2_1$ space group. The crystal data are as follows: $a = 22.4933(14)$, $b = 9.1067(7)$, $c = 10.6450(5)$ Å and $V = 2180.5(2)$ Å^3. Complex **II** takes nine-coordinated structure with a monocapped square antiprism, and crystallizing in the monoclinic crystal system with $P2_1/c$ space group. The cell dimensions are as follows: $a = 12.9600(11)$, $b = 12.6209(12)$, $c = 16.9151(15)$ Å, $\beta = 122.021(2)°$ and $V = 2345.8(4)$ Å^3. Each ethylenediammonium (EnH_2^{2+}) cation in (EnH_2)[Y^{III}(Egta)H_2O]$_2$ · $6H_2O$ (**II**) connects three adjacent [Y^{III}(Egta)(H_2O)]$_2^{2-}$ anions through hydrogen bonds. While in **II**, there are two types of EnH_2^{2+} cations, which form hydrogen bonds with the neighboring [Y^{III}(Egta)(H_2O)]$_2^{2-}$ anions, leading to the formation of a 2D ladder-like layer structure. The results showed that the ionic radius of rare earth metals play a crucial role in crystal and molecular structure of their complexes.

DOI: 10.1134/S1070328416030040

INTRODUCTION

Within recent years, due to the unique physical and chemical properties of lanthanide ions, lanthanide complexes are of great importance in industrial, chemical, medical, and sensor applications [1, 2]. In particular, rare earth complexes are applied as magnetic resonance imaging (MRI) contrast agent [3, 4], shift reagents for NMR spectroscopy [5], luminescent chemosensors and probes for medical diagnostics [6–9]. For instance, some Tb(III) and Eu(III) complexes with aminopolycarboxylic acid ligands have unusual spectroscopic characteristics including millisecond excited-state lifetime, sharply spiked emission spectra (few nm), and large Stokes shifts (>150 nm), so they have been used as probes in fluoroimmunoassay [10, 11], and as sensors for certain bioactive ions [12]. Moreover, Nd(III) complexes have good anti-inflammation activity, and Gd(III) complexes are used as contrast agents in MRI [13–16]. The $4f(^1G_4)$–$4f(^3H_6)$ electronic transition of Tm^{3+} provides a spectrally narrow blue light emission at about 480 nm [17], and this will benefit full-color flat display. What's more, the Y^{3+} ion as a radioactive rare earth metal ion can emit appropriate rays, thus, many radioactive ^{90}Y compounds are used for treatment of many kind of cancer [18]. In addition, high energy β-emitter of Y(III) represents significant superiority in the treatment of larger tumor [19, 20]. Recently, many researchers have focused on the Lu(III) complexes for their interesting properties. For instance, $^{177}LuCl_3$ are effective in curing small tumors that just begin malignant lesions. Hence, this maks Lu(III) and Y(III) complexes with aminopolycarboxylic acid ligands have important application in the field of medicine. Of course, these applications all are based on the understanding of the characters of the rare-earth or radioactive rare-earth metal complexes in detail.

For these reasons given above, it is necessary to determine the crystal and molecular structures of rare-earth metal complexes with aminopolycarboxylic acids. Hence, we contribute to this basic research, so that making good use of the complexes of rare-earth metal ions with aminopolycarboxylic acids. As it is well known, rare earth metal ions can form eight-,

[1] The article is published in the original.

nine- and ten-coordinate complexes with various aminopolycarboxylic acid ligands comparing to transition metal ions [21–25]. So, as one of rare-earth metal ions, the Y^{3+} ion conforms to this rule. By comparative previous research, it was found that the coordination number of Y(III) complexes can adopt eight or nine. For instance, $(NH_4)_3[Y^{III}(Nta)_2]$ [26] and $Na[Y^{III}(Cydta)(H_2O)_2] \cdot 5H_2O$ [27] were eight-coordinate structures, while $\{K[Y^{III}(Egta) \cdot 4H_2O\}_n$ (**III**) [26] and $Na[Y^{III}(Edta)(H_2O)_3] \cdot 5H_2O$ [27] both adopt nine-coordinate structure. For the Y^{3+} ion, due to its relatively small radius (1.040 Å) and electronic configuration (d^0) among rare-earth metal ions, there is a little chance to form ten-coordinate complexes. Furthermore, the Lu^{3+} ions with small ionic radii and more *f*-orbital electrons (f^{14}) form only eight-coordinate complexes [28, 29]. According to above mentioned, the Y(III) complex with Egta ligands and ethylenediamine should form a nine-coordinate structure, and Lu(III) complex with Egta ligands and ethylenediamine should adopt an eight-coordinate structure. Therefore, different rare earth metal ions the effects upon coordination number, coordinate structure, molecular structure and crystal structure.

In order to validate this supposition and extend our work, fortunately, two novel rare earth metal complex with Egta ligand namely, $(EnH)[Lu^{III}(Egta)] \cdot 2H_2O$ (**I**) and $(EnH_2)[Y^{III}(Egta)(H_2O)]_2 \cdot 6H_2O$ (**II**), were successfully synthesized and detected. As expected, **I** adopts an eight-coordinate structure with the square antiprism (SAP) configuration, and **II** adopts nine-coordinate monocapped square antiprisms (MCSAP) with monoclinic space group $P2_1/c$. However, due to the different rare earth metal ion, **I** and **II** have also some differenences in coordinate structure, molecular structure and space group and so on. In addition, this study supports the idea that the structures of the rare earth metal complexes with aminopolycarboxylic acid are mainly determined by the radii of the central metal ions as mentioned above, ligand structure and counter ion. Nevertheless, **II**, being different from **I**, adopts 2D ladder-like network through hydrogen bonds formed between ethylenediamine and $[Y^{III}(Egta)(H_2O)]_2^{2-}$ (Egta = ethyleneglycol-bis-(2-aminoethylether)-*N*,*N*,*N*',*N*'-tetraacetic acid) complex anions. Hence, the radii of the central metal ions species have vital effect on the coordinate structure, molecular structures and crystal structure.

EXPERIMENTAL

Materials and methods. Lu_2O_3 powder (99.999%, Yuelong Rare Earth Co., Ltd., China), Y_2O_3 powder (99.999%, Yuelong Rare Earth Co., Ltd., China) and ligand of H_4Egta (A.R., Beijing SHLHT Science & Trade Co., Ltd., China) were used to synthesize the title aminopolycarboxylic acid complexes. In addition, ethylenediamine (En) aqueous solution was slowly added to above solution in order to adjust the pH to 6.0. The structure of complexes were detected by X-ray equipment (XT-V130, Beijing Xinzhuo, Company, China).

Synthesis of I. H_4Egta (A.R., Beijing SHLHT Science & Trade Co., Ltd., China) (1.9017 g, 5.0 mmol) was added to 100 mL warm water and Lu_2O_3 powder (99.999%, Yuelong Rare Earth Co., Ltd., China) (0.9852 g, 2.5 mmol) was slowly added to above solution. After the mixture had been stirred and refluxed for 18.0 h, the solution became transparent. And then the pH value was also adjusted to 6.0 by dilute En aqueous solution. Finally, the solution was concentrated to 25 mL. A light yellow crystal appeared after three weeks at room temperature. The yield is 2.59 g (79.86%).

Synthesis of II. H_4Egta (1.9017 g, 5.0 mmol) was added to 100 mL warm water and Y_2O_3 powder (99.999%, Yuelong Rare Earth Co., Ltd., China) (0.9852 g, 2.5 mmol) was slowly added to above solution. After the mixture had been stirred and refluxed for 18.0 h, the solution became transparent. And then the pH value was also adjusted to 6.0 by dilute En aqueous solution. Finally, the solution was concentrated to 25 mL. A light-yellow crystal appeared after two weeks at room temperature. The yield is 2.45 g (86.25%).

X-ray structure determination. X-ray intensity data of **I** and **II** samples were collected on a Bruker SMART CCD type X-ray diffractometer system with graphite-monochromatized Mo*K* radiation (λ = 0.71073 Å) using φ–ω scan technique in the range of $1.72° \leqslant \theta \leqslant 26.00°$. Their structures were solved by direct methods. All non-hydrogen atoms were refined anisotropically by full-matrix least-squares methods on F^2. All the calculations were performed by the SHELXTL-97 program on PDP11/44 and Pentium MMX/166 computers. The crystal data and structure refinement for two complexes were listed in Table 1. And the selected bond distances and bond angles of two complexes were listed in Table 2.

Supplementary material has been deposited with the Cambridge Crystallographic Data Centre (nos. 966211 (**I**) and 966210 (**II**); deposit@ccdc.cam.ac.uk or http://www.ccdc.cam.ac.uk).

RESULTS AND DISCUSSION

The comparison of FT-IR spectra between H_4Egta and **I** are shown in Figs. 1a, 1b. It reveals that the ν(C–N) of **I** appears at 1055 cm^{-1}, which displays red-shifts by 80 cm^{-1} compared with that (1135 cm^{-1}) of H_4Egta. This suggests that the amine nitrogen atoms of the H_4Egta ligand are coordinated to the Lu^{3+} ion. The spectrum of free H_4Egta ligand shows strong absorp-

Table 1. Crystallographic data and structure refinement details for **I** and **II**

Parameter	Value	
	I	**II**
Empirical formula	$C_{16}H_{33}N_4O_{12}Lu$	$C_{15}H_{33}N_3O_{14}Y$
Formula weight	648.43	568.35
Temperature, K	293(2)	298(2)
Crystal system	Orthorhombic	Monoclinc
Space group	$Pca2_1$	$P2_1/c$
Unit cell dimensions		
a, Å	22.4933(14)	12.9600(11)
b, Å	9.1067(7)	12.6209(12)
c, Å	10.6450(5)	16.9151(15)
β, deg	90	122.021(2)
Volume, Å^3	2180.5(2)	2345.8(4)
Z	4	4
ρ_{calcd}, mg/m^3	1.975	1.609
Absorption coefficient, mm^{-1}	4.599	2.559
F(000)	1296	1180
Crystal size, mm	0.35 × 0.17 × 0.13	0.24 × 0.15 × 0.11
θ Range for data collection, deg	2.63–25.02	2.43–25.01
Limiting indices	$-17 \leqslant h \leqslant 26$	$-12 \leqslant h \leqslant 15$
	$-10 \leqslant k \leqslant 10$	$-14 \leqslant k \leqslant 15$
	$-12 \leqslant l \leqslant 12$	$-20 \leqslant l \leqslant 11$
Reflections collected	13383	11427
Independent reflections (R_{int})	3789 (0.0801)	4131 (0.0947)
Completeness to θ_{max}, %	99.9	99.8
Max and min transmission	0.5862 and 0.2959	0.7661 and 0.5787
Goodness-of-fit on F^2	1.050	1.009
Final R indices ($I > 2\sigma(I)$)	$R_1 = 0.0680$, $wR_2 = 0.1799$	$R_1 = 0.0656$, $wR_2 = 0.1539$
R indices (all data)	$R_1 = 0.0960$, $wR_2 = 0.2090$	$R_1 = 0.1110$, $wR_2 = 0.1772$
Largest difference peak and hole, e Å^{-3}	2.991 and −1.737	1.565 and −0.957
Absorption correction	Empirical	

tion band around 1735 cm^{-1} originating from stretching vibrations of carbonyl group ν(C=O), which disappears completely in the FT-IR spectrum of the complex **I**. Furthermore, **I** gives the characteristic absorption peaks of carboxyl groups at 1619 cm^{-1} for the asymmetric stretching vibration, revealing a red-shift (18 cm^{-1}) compared with 1637 cm^{-1} of H_4Egta. The ν_s(COO) band of **II** appears at 1403 cm^{-1}, showing a blue-shift (8 cm^{-1}) compared with that (1397 cm^{-1}) of H_4Egta. These changes in the peak position confirm that the oxygen atoms from the carboxyl groups are also coordinated to the Lu^{3+} ion. Besides, there is a broad absorption band near 3479 cm^{-1} for **I**. It could be reasonably attributed to the stretching vibration absorption peak of O–H bond.

Similarly, the IR spectra of complex II (Fig. 1c) reveals that the ν(C–N) of **II** appears at 1092 cm^{-1}, which displays a red-shift (43 cm^{-1}) compared with that (1135 cm^{-1}) of H_4Egta, indicating that the amine nitrogen atoms of H_4Egta ligand are coordinated to the Y^{3+} ion. The ν_{as}(COOH) band of H_4Egta at 1735 cm^{-1} disappears in the FT-IR spectrum of the complex **II**. Also, it can be found that ν_{as}(COO) band of the complex **II** appears at 1610 cm^{-1}, revealing a red-shift (27 cm^{-1}) compared with 1637 cm^{-1} of H_4Egta, and the ν_s(COO) band of II appears at

Table 2. Selected bond distances (Å) and angles (deg) of **I** and **II**

Bond	*d*, Å	Bond	*d*, Å	Bond	*d*, Å
		I			
Lu(1)–O(1)	2.332(18)	Lu(1)–O(5)	2.27(2)	Lu(1)–N(1)	2.46(3)
Lu(1)–O(2)	2.42(2)	Lu(1)–O(7)	2.241(14)	Lu(1)–N(2)	2.52(2)
Lu(1)–O(3)	2.20(2)	Lu(1)–O(9)	2.22(2)		
		II			
Y(1)–O(1)	2.463(4)	Y(1)–O(5)	2.331(4)	Y(1)–O(11)	2.425(4)
Y(1)–O(2)	2.475(4)	Y(1)–O(7)	2.334(4)	Y(1)–N(1)	2.629(5)
Y(1)–O(3)	2.318(4)	Y(1)–O(9)	2.327(4)	Y(1)–N(2)	2.620(5)
Angle	ω, deg	Angle	ω, deg	Angle	ω, deg
		I			
O(1)Lu(1)O(2)	66.4(12)	O(2)Lu(1)O(9)	134.7(7)	O(5)Lu(1)N(1)	68.1(6)
O(1)Lu(1)O(3)	79.5(13)	O(2)Lu(1)N(1)	124.1(9)	O(5)Lu(1)N(2)	75.3(8)
O(1)Lu(1)O(5)	91.7(9)	O(2)Lu(1)N(2)	68.0(8)	O(7)Lu(1)O(9)	96.7(7)
O(1)Lu(1)O(7)	97.2(6)	O(3)Lu(1)O(5)	138.0(8)	O(7)Lu(1)N(1)	145.0(11)
O(1)Lu(1)O(9)	156.8(10)	O(3)Lu(1)O(7)	75.0(11)	O(7)Lu(1)N(2)	75.7(10)
O(1)Lu(1)N(1)	74.0(10)	O(3)Lu(1)O(9)	86.3(8)	O(9)Lu(1)N(1)	84.0(8)
O(1)Lu(1)N(2)	134.4(12)	O(3)Lu(1)N(1)	70.0(8)	O(9)Lu(1)N(2)	67.4(7)
O(2)Lu(1)O(3)	134.0(10)	O(3)Lu(1)N(2)	137.5(8)	N(1)Lu(1)N(2)	134.5(8)
O(2)Lu(1)O(5)	75.1(8)	O(5)Lu(1)O(7)	146.9(11)		
O(2)Lu(1)O(7)	79.4(9)	O(5)Lu(1)O(9)	86.6(8)		
		II			
O(1)Y(1)O(2)	67.35(14)	O(2)Y(1)O(11)	77.67(15)	O(5)Y(1)N(1)	65.54(14)
O(1)Y(1)O(3)	99.30(15)	O(2)Y(1)N(1)	124.65(15)	O(5)Y(1)N(2)	75.84(14)
O(1)Y(1)O(5)	71.99(14)	O(2)Y(1)N(2)	68.05(15)	O(7)Y(1)O(9)	89.37(15)
O(1)Y(1)O(7)	137.63(14)	O(3)Y(1)O(5)	130.13(14)	O(7)Y(1)O(11)	148.54(15)
O(1)Y(1)O(9)	132.70(15)	O(3)Y(1)O(7)	79.96(15)	O(7)Y(1)N(1)	73.99(15)
O(1)Y(1)O(11)	65.36(14)	O(3)Y(1)O(9)	81.03(14)	O(7)Y(1)N(2)	63.95(15)
O(1)Y(1)N(1)	67.52(15)	O(3)Y(1)O(11)	74.04(15)	O(9)Y(1)O(11)	69.53(14)
O(1)Y(1)N(2)	131.16(15)	O(3)Y(1)N(1)	65.91(14)	O(9)Y(1)N(1)	144.86(16)
O(2)Y(1)O(3)	151.70(16)	O(3)Y(1)N(2)	129.54(15)	O(9)Y(1)N(2)	65.39(14)
O(2)Y(1)O(5)	71.31(15)	O(5)Y(1)O(7)	76.57(15)	O(11)Y(1)N(1)	109.92(15)
O(2)Y(1)O(7)	127.08(15)	O(5)Y(1)O(9)	141.05(14)	O(11)Y(1)N(2)	121.96(15)
O(2)Y(1)O(9)	90.16(15)	O(5)Y(1)O(11)	134.29(14)	N(1)Y(1)N(2)	128.03(16)

1401 cm^{-1}, showing a blue-shift (6 cm^{-1}) compared with 1395 cm^{-1} of H_4Egta. These results clearly show that oxygen in carboxylates participate in coordination to Y(III). Also, a strong and wide absorption band around 3462 cm^{-1} in **II** could be reasonably assigned to O–H stretch.

As shown in Fig. 2a, the TG curve of **I** roughly shows a three-stage decomposition pattern. The first stage weight loss is about 7.434% from room temperature to 184°C, which corresponds to release of En. The second weight loss of 5.25% from 184 to 308°C should correspond to the expulsion of two crystal waters. The last stage weight loss is attributed to the decomposition of the organic ligand starting from 308 to 800°C, the weight loss ratio is about 42.38%. The final residue is mainly Lu_2O_3, the overall weight loss ratio is about 65.07% according to the mass calculation.

The thermal decomposition process of **II** complex displays similar thermal behavior with **I**, but it has four stages. It is found in Fig. 2b that the first thermal decomposition happens from 25 to 116°C. In this step the weight loss ratio is about 10.53%, which corresponds to the releasing six lattice water molecules. The second weight loss of 2.65% from 116 to 139°C corre-

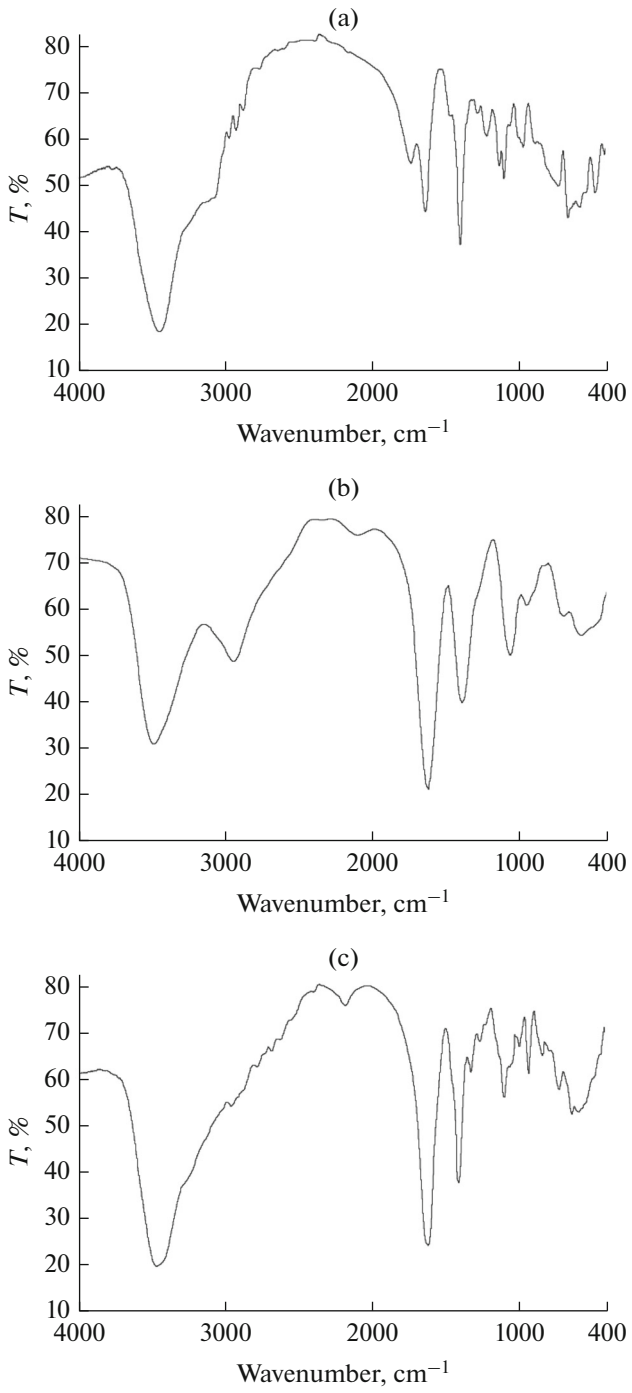

Fig. 1. IR spectra of H_4Egta (a), **I** (b), and **II** (c).

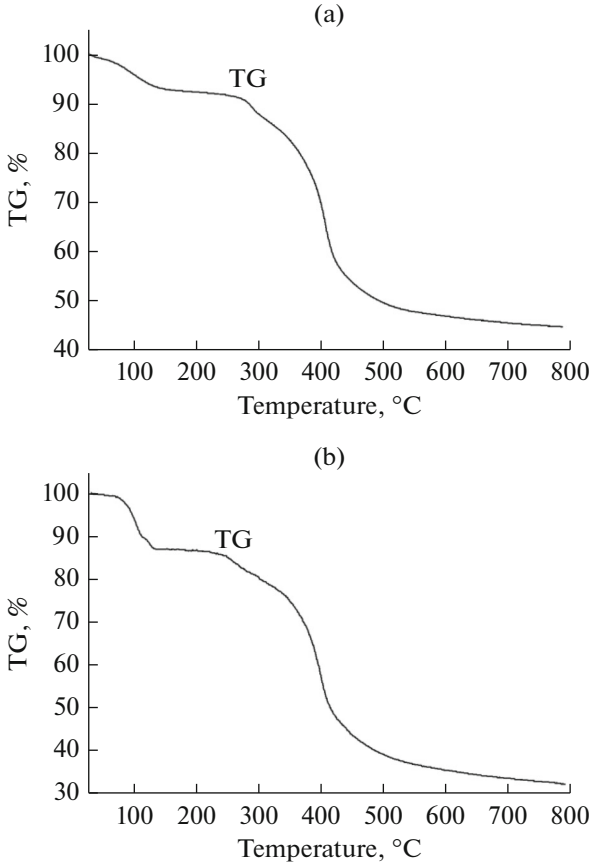

Fig. 2. TG–DTA curves of **I** (a) and **II** (b).

sponds to the releases of two coordinated water molecules. The third stage weight loss (6.04%) from 139 to 295°C corresponds to the expulsion En. Then, the sample decomposes gradually and the decomposition is completed at 800°C. The corresponding weight loss is about 48.65%, and the corresponding final remainder is mainly Y_2O_3. The total weight loss ratio is about 67.87% according to the mass calculation.

Figure 3a exhibits that Lu(III) forms (1 : 1) eight-coordinate complex with the Egta ligand, which is different from many other rare-earth complexes with aminopolycarboxylic acid ligands. The reason that the Lu(III) adopts an eight-coordinate conformation due to its slightly small ionic radius and more *f*-orbital electrons, which generates a relatively small coordination number. It has a mononuclear molecular structure. The center metal Lu^{3+} ion in **I** is surrounded by two amine N atoms (N(1) and N(2)) and six carboxylic O atoms (O(1), O(2), O(3), O(5), O(7) and O(9)), all come from one H_4Egta ligand. The two N atoms and six O atoms of one Egta ligand create seven five-membered chelating rings with the central Lu^{3+} ion, in which the four atoms are almost coplanar in each ring.

Obviously, the Lu^{3+} ion in this $[Lu^{III}(Egta)]^-$ complex anion is mononuclear eight-coordinate geometry with distorted SAP conformation (Fig. 4a). This is different from $(EnH_2)[Er^{III}(Egta)(H_2O)]_2 \cdot 6H_2O$ (**IV**) [30] and $(EnH_2)[Ho^{III}(Egta)(H_2O)]_2 \cdot 6H_2O$ (**V**) [31], whose coordinate geometry around Er^{3+} or Ho^{3+} all adopt a nine-coordinate pseudo-MCSAP conformation. In the coordinate atoms around Lu, the set of O(3), O(7), O(9) and N(2) and the set of O(1), O(2),

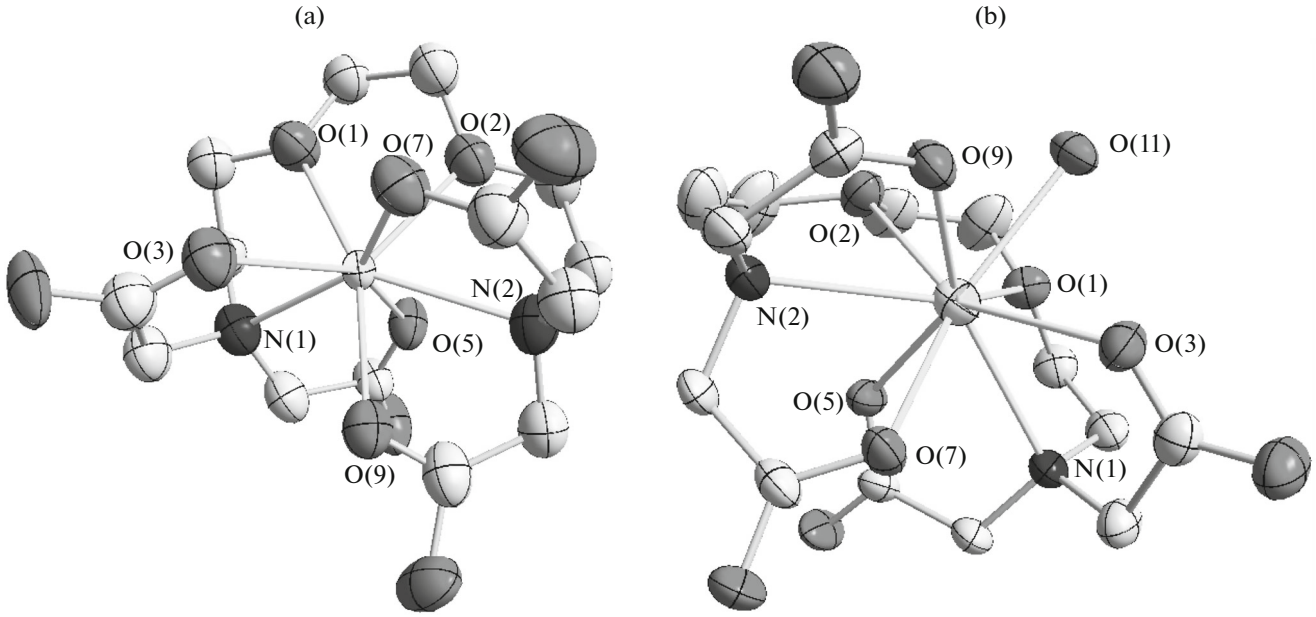

Fig. 3. Molecular structures of **I** (a) and **II** (b).

O(5) and N(1) form two approximate square (top and bottom) planes, respectively, which are basically parallel to each other and the torsion angle is about 45°. Furthermore, the upper quadrilateral plane is formed by three carboxyl O atoms (O(3), O(7) and O(9)) and one amine N atom (N(2)), the bottom quadrilateral plane is formed by one carboxyl O atom (O(5)), two ethyleneglycol O atoms (O(1) and O(2)) and one amine N atoms (N(1)). Furthermore, there is no capped atom in the geometric configuration of **I**. This means that no repulsion to the top or bottom square plane could yield. Therefore, it is distorted slightly in the coordination geometry of the $[Lu^{III}(Egta)]^-$ complex anion, and the coordination geometry is close to a standard square antiprismatic conformation. In addition, from Fig. 4a, it can be calculated that the value of the square antiprism angle, to the upper quadrilateral plane, the average value of the trigonal dihe-

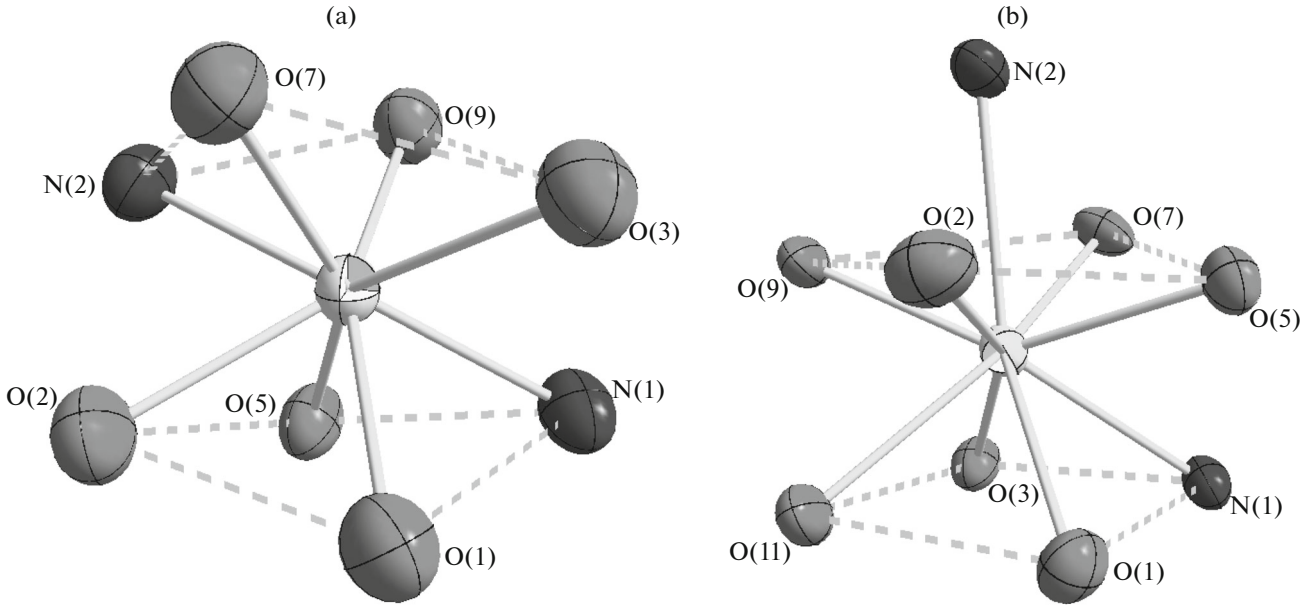

Fig. 4. Coordination polyhedrons around Lu^{3+} ion in **I** (a) and Y^{3+} ion in **II** (b).

Table 3. Geometric parameters of hydrogen bonds of **II**

D–H··· A	Distance, Å			Angle	Symmetry code
	D–H	H···A	D···A	DHA, deg	
N(3)–H(3*A*)···O(8)	0.89	1.88	2.770	177	$-x+1, y+1/2, -z+1/2$
N(3)–H(3*B*)···O(10)	0.89	1.89	2.771	171	$-x+1, -y+1, -z+1$
N(3)–H(3*B*···O(9)	0.89	2.55	3.039	115	$-x+1, -y+1, -z+1$
N(3)–H(3*C*)···O(4)	0.89	1.91	2.771	163	

dral angle between Δ(N(2)O(9)O(7)) and Δ(O(9)O(7)O(3)) is about 21.42°, and between Δ(O(9)N(2)O(3)) and Δ(N(2)O(3)O(7)) is about 25.78°. To the bottom plane, the value of the dihedral angle between Δ(O(2)O(5)O(1)) and Δ(O(5)O(1)N(1)) triangles is 24.26°, and between Δ(O(5)O(2)N(1)) and Δ(O(2)N(1)O(1)) triangle it is 21.27°. According to these calculated data, which are smaller than 26.4°, we can firmly draw a conclusion that the conformation of $Lu(1)N_2O_6$ in the $[Lu^{III}(Egta)]^-$ complex anion indeed keeps a SAP conformation but distort to some extent.

As shown in Table 2, for **I**, the Lu(1)–O bond distances vary from 2.20(2) Å (Lu(1)–O(3)) to 2.42(2) Å (Lu(1)–O(2)). Furthermore, the bond distances of Lu(1)–O(1) and Lu(1)–O(2) (both belonging to ethyleneglycol O atoms) are somewhat longer than other Lu(1)–O bond lengths, which indicates that the O atoms (O(3), O(5) and O(7)) from coordinate carboxylic more stably than ethyleneglycol O atoms (O(1) and O(2)). This is consistent with the findings with H_4Egta ligands made by previously reported. While the Lu(1)–N bond distances range from 2.46(3) Å (Lu(1)–N(1)) to 2.52(2) Å (Lu(1)–N(2)). From the above, we can come to the conclusion that Lu(1)–O bonds are much stable than Lu(1)–N bonds. Table 2 also shows a series of bond angles, for instance, the OLu(1)O bond angles in **I** is range from 66.4(12)° (O(1)Lu(1)O(2)) to 156.8(10)° (O(1)Lu(1)O(9)), OLu(1)N bond angles vary from 67.4(7)° (O(9)Lu(1)N(2)) to 145.0(11)° (O(7)Lu(1)N(1)), and the NLu(1)N bond angles is 134.5(8)°. Among them, the largest angle is 156.8(10)° (O(1)Lu(1)O(9)) and the smallest bond angle is 66.4(12)° (O(1)Lu(1)O(2)). The reason might be that the O(1) atom forms hydrogen bond with the adjacent crystal water molecule. According to these data, we can draw a conclude, although there are some distorted, the conformation around Lu(1) indeed keeps a SAP conformation.

In one unit cell, as shown in Fig. 5a, there are four molecules of **I** in a unit cell. The complex molecules connect with each other through hydrogen bonding and protonated cation (EnH^+). Therefore, as a whole crystal, a network structure is formed through hydrogen bonds and electrostatic bonding. In addition, the hydrogen bonds play an important role in the structure of **I**. As seen from Fig. 6a, the EnH^+ cation is located in a center symmetric structure. Obviously, each cation (EnH^+) with three adjacent $[Lu^{III}(Egta)]^-$ complex anions forms hydrogen bonds. That is, N(3) connects three O atoms (O(4), O(8) and O(10)), in which O(4), O(8) and O(10) all come from three different carboxyl group of three $[Lu^{III}(Egta)]^-$ complex anions, respectively. However, N(4) connects four O atoms (O(4), O(7), O(8) and O(10)), in which O(7) and O(8) come from a same carboxyl group of one $[Lu^{III}(Egta)]^-$ complex anion, and then O(4) and O(10) come from two different carboxyl group of two neighboring $[Lu^{III}(Egta)]^-$ complex anions, respec-

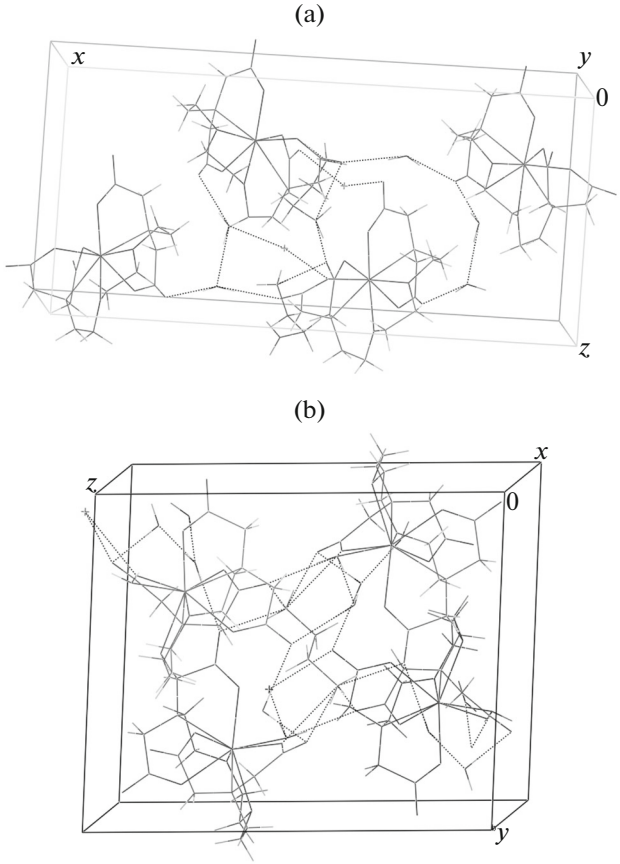

Fig. 5. Arrangements of of **I** (a) and **II** (b) in unit cell (dashed lines represent intermolecular hydrogen bonds).

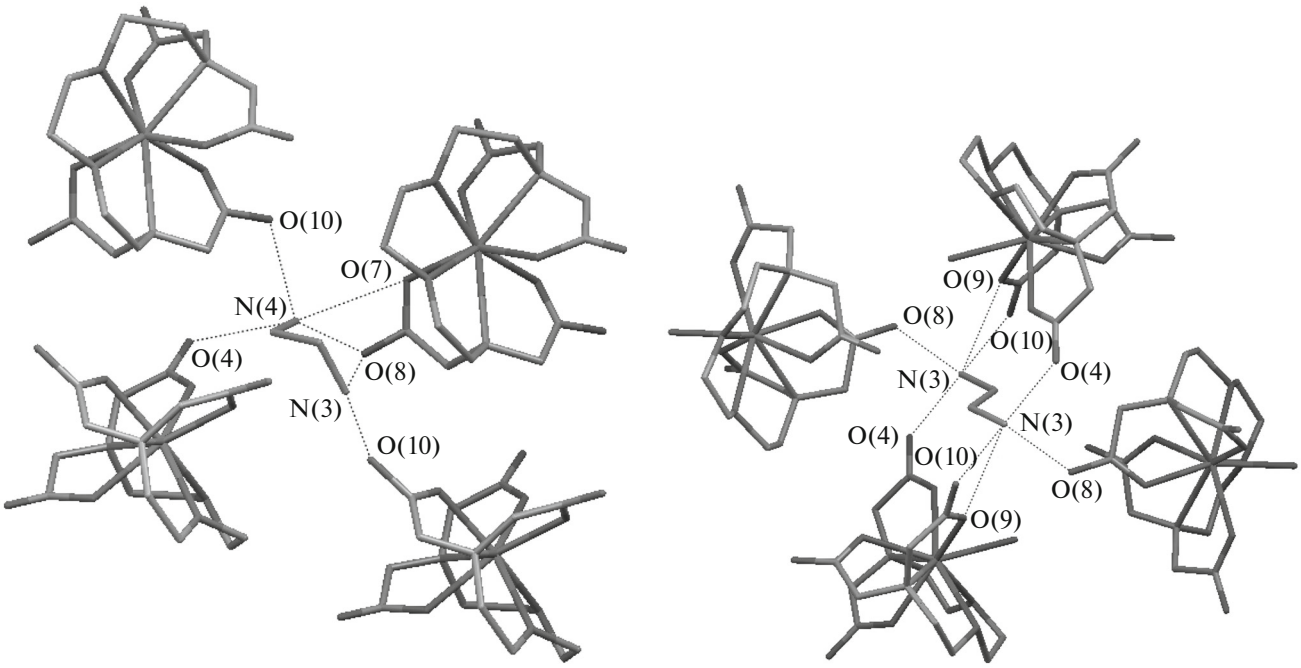

Fig. 6. Bindings between EnH_2^{2+} and $[Y^{III}(Egta)H_2O]^-$ in **I** (a) and **II** (b) (dashed lines represent intermolecular hydrogen bonds).

tively. It is worth reminding that the O(8) connects with N(3) and N(4) atoms as a simultaneity.

The nine-coordinated molecular structure of **II** with a 1 : 1 proportion of rare earth metal ions to ligand stoichiometry shown in Fig. 3b. Its molecular and crystal structures are different in respect to **I** mentioned above. However, it is similar to the findings that previously have been reported, for instance, **IV**, **V** and $(EnH_2)[Sm^{III}(Egta)H_2O]_2 \cdot 6H_2O$ [32]. Figure 3b has also shown the molecular structure of **II** complex. The central Y^{3+} ion is nine-coordinated with one H_4Egta ligand by two nitrogen atoms and six carboxylic oxygen atoms, which come from the same H_4Egta ligand, and another oxygen atom from water molecules. Unlike the complex of **I**, excepting water molecule, the eight atoms from one octadentate H_4Egta ligand shape seven structurally stable five-member rings with Y^{3+} ion as well as the atoms in each five-member ring are almost coplanar. The finding is consistent with previously reported.

Evidently, the coordination geometry around the central Y^{3+} ion in $[Y^{III}(Egta)(H_2O)]_2^{2-}$ complex anion is a nine-coordinate distorted MCSAP (Fig. 4b) with seven chelating five-membered rings. Furthermore, the capping donor atom N(2) locates the above quadrilateral plane. The above quadrilateral plane of antiprism is formed by three carboxyl O atoms (O(5), O(7) and O(9)) and one ethyleneglycol O atom (O(2)). While the bottom quadrilateral plane is done by one amine N atom (N(1)), one ethyleneglycol O atom (O(1)), one carboxyl O atom (O(3)) and one coordinate water O atom (O(11)). In addition, it also can be found that the $Y(III)N_2O_7$ part is not standard MCSAP (see Fig. 4b). To the upper plane, the average value of the MCSAP angle between Δ(O(5)O(2)O(7)) and Δ(O(2)O(7)O(9)) is about 12.64°, and between Δ(O(2)O(5)O(9)) and Δ(O(5)O(9)O(7)) is about 12.58°. The nether plane, the average value of the MCSAP angle between Δ(O(1)N(1)O(11)) and Δ(N(1)O(11)O(3)) is about 6.26°, and between Δ(O(3)O(1)N(2)) and Δ(O(11)O(3)O(1)) is about 5.51°. According to these calculated data and Guggenberger and Muetterties' method [33], we may safely come to conclusion that the conformation of $Y(III)N_2O_7$ in $[Y^{III}(Egta)(H_2O)]_2^{2-}$ complex anion indeed keeps a pseudo-MCSAP polyhedron but distorted to a small extent. The conclusion is consistent with other Y(III) complexes with aminopolycarboxylic acid ligands, for instance, complex **III**.

The series of bond distances for **II** are given in Table 2. The lengths of all Y(1)–O bonds are in the wide varying from 2.318(3) Å (Y(1)–O(3)) to 2.478(4) Å (Y(1)–O(2)) with an average value of 2.382(6) Å. By comparison it can be found that, bond distances for **II** is somewhat longer than the corresponding value (2.20(2) to 2.42(2) Å) in **I**, indicating that the complex of **I** is more stable than **II**. While the two Y(1)–N bond distances are 2.620(5) Å (Y(1)–N(2)) and 2.629(5) Å (Y(1)–N(1)), with an average value of 2.6245(7) Å. This is in agreement with the average lengths of general nine-coordinate Y(III)–O

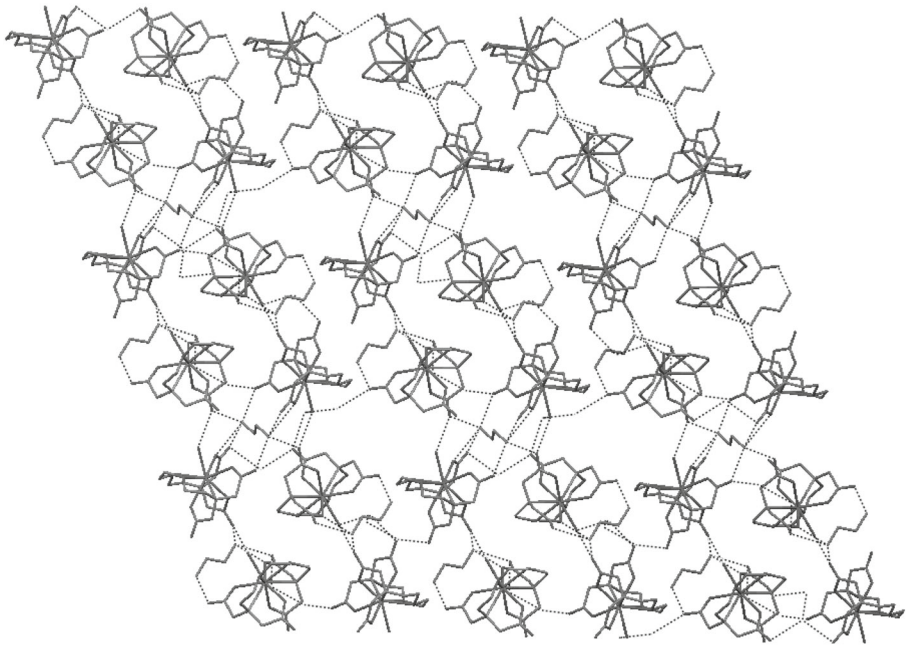

Fig. 7. Polyhedral view of the 2D ladder-like layered network of **II**.

and Y(III)–N bonds. So, we firmly conclude that the O atoms coordinate to the central Y^{3+} ion much stronger than the N atoms, since Y(III)–N bond lengths are significantly longer than the Y(III)–O bond lengths. In addition, Table 2 illustrates a series of bond angles. The OYO bond angles are placed changing from 65.36(14)° (O(1)Y(1)O(11)) to 151.70(16)° (O(2)Y(1)O(3)). The OYN bond angles vary from 63.95(15)° (O(7)Y(1)N(2)) to 144.86(16)° (O(9)Y(1)N(1)), and the N(1)YN(2) bond angle is 128.03(16)°. Among them, the smallest and largest bond angles are 63.95(15)° (O(7)Y(1)N(2)) and 151.70(16)° (O(2)Y(1)O(3)), respectively. The reason might be that O(1) and O(7) atoms form hydrogen bond with the adjacent crystal water molecule. Thus, all these obviously distort the geometrical configuration of $Y(III)N_2O_7$ part in $[Y^{III}(Egta)(H_2O)]_2^{2-}$.

In one unit cell, as seen in Fig. 5b, there are four II molecules. The molecules connect with each other through hydrogen bonds and electrostatic forces with crystallization water and protonated ethylenediamine cation (EnH_2^{2+}). In addtion, the hydrogen bonds play an important role in the construction of 2D ladder-like network structure of **II**. As seen from Fig. 6b, the cation (EnH_2^{2+}) is located in a center symmetric structure, and the symmetric center is in the middle position of the ethylene, which is exactly same as previous complexes. Obviously, the cation ($EnH_2{}^{2+}$) with three adjacent $[Y^{III}(Egta)(H_2O)]_2^{2-}$ complex anions forms hydrogen bonds. That is, each N(3) connect with four carboxyl O atoms (O(4), O(8), O(9) and O(10)), in which O(4), O(9) and O(10) come from a same carboxyl group of one $[Y^{III}(Egta)(H_2O)]_2^{2-}$ complex anion, and O(8) comes from adjacent carboxyl group of $[Y^{III}(Egta)(H_2O)]_2^{2-}$ complex anion. The hydrogen bond distances of N(3)···O(4), N(3)···O(8), N(3)···O(9), and N(3)···O(10) are 2.771, 2.770, 3.039, and 2.771 Å, respectively (Table 3). Shown in Fig. 6b, every four $[Y^{III}(Egta)(H_2O)]_2^{2-}$ complex anions are interconnected together by sharing ethylenediamine (N(3)–C(15)–C(15)–N(3)), forming a basic SBU (secondary building units). The two neighboring SBU are further linked leading to the formation of 2D network in plane, which is shown in Fig. 7. Owing to the special coordination environment, the Newman' pattern dihedral angle of En is closely 180°. So, four atoms of En locate in the same plane. Therefore, it can be concluded that amino acids as a part of protein can interact with $[Y^{III}(Egta)(H_2O)]_2^{2-}$ complex anion by different binding manner.

ACKNOWLEDGMENTS

The authors greatly acknowledge the National Science Foundation of China (21371084), Shenyang Science and Technology Plan Project (F13-289-1-00), Key Laboratory Basic Research Foundation of Liaoning Provincial Education Department (L2015043) and Liaoning Provincial Department of Education Innovation Team Projects (LT2015012) for financial sup-

port. The authors also thank our colleagues and other students for their participating in this work.

REFERENCES

1. Bünzli, J.C.G. and Piguet, C., *Chem. Rev.*, 2002, vol. 102, p. 1897.
2. Tsukube, H. and Shinoda, S., *Chem. Rev.*, 2002, vol. 102, p. 2389.
3. Laurent, S., Vander Elst, L., Wautier, M., et al., *Bioorg. Med. Chem. Lett.*, 2007, vol. 17, p. 6230.
4. Sink, R.M., Buster, D.C., and Sherry, A.D., *Inorg. Chem.*, 1990, vol. 29, p. 3654.
5. Takahashi, K., Nakamura, H., Furumoto, S., et al., *Bioorg. Med. Chem.*, 2005, vol. 13, p. 735.
6. Li, L., Yang, J.H., Wu, X., et al., *Talanta*, 2005, vol. 65, p. 201.
7. Law, G.L., Wong, K.L., Man, C.W.Y., et al., *J. Am. Chem. Soc.*, 2008, vol. 130, p. 3714.
8. Wong, K.L., Law, G.L., Murphy, M.B., et al., *Inorg. Chem.*, 2008, vol. 47, p. 5190.
9. Zheng, S.L., Tong, M.L., and Chen, X.M., *Coord. Chem. Rev.*, 2003, vol. 246, p. 185.
10. Volkert, W.A., Goeckeler, W.F., Ehrhardt, G.J., et al., *J. Nucl. Med.*, 1991, vol. 32, p. 174.
11. Ozolinsh, M. and Eichler, H.J., *Appl. Phys. Lett.*, 2000, vol. 77, p. 615.
12. Terai, T., Kikuchi, K., Iwasawa, S., et al., *J. Am. Chem. Soc.*, 2006, vol. 128, p. 6928.
13. Lauffer, R.B., *Chem. Rev.*, 1987, vol. 87, p. 901.
14. Aime, S., Botta, M., Fasano, M., et al., *Chem. Soc. Rev.*, 1998, vol. 27, p. 19.
15. Accardo, A., Tesauro, D., Aloj, L., et al., *Coord. Chem. Rev.*, 2009, vol. 253, p. 179.
16. Alexander, V., *Chem. Rev.*, 1995, vol. 95, p. 273.
17. Hong, Z.R., Li, W.L., Zhao, D.X., et al., *Synth. Met.*, 1999, vol. 104, p. 165.
18. Stein, R., Chen, S., Reed, L., et al., *Cancer*, 2002, vol. 94, p. 51.
19. Hak, S., Sanders, H.M.H.F., Agrawal, P., et al., *Eur. J. Pharm. Biopharm.*, 2009, vol. 72, p. 397.
20. Li, Z.F., Li, W.S., Li, X.J., et al., *Magn. Reson. Imaging*, 2007, vol. 25, p. 412.
21. Wang, J., Zhang, X.D., Ling, X., et al., *J. Mol. Struct.*, 2002, vol. 610, p. 151.
22. Wang, J., Zhang, X.D., Liu, Z.R., et al., *J. Mol. Struct.*, 2002, vol. 613, p. 189.
23. Wang, J., Liu, Z.R., Zhang, X.D., et al., *J. Mol. Struct.*, 2003, vol. 644, p. 29.
24. Wang, X.F., Wang, J., Gao, J., et al., *Russ. J. Coord. Chem.*, 2008, vol. 34, p. 350.
25. Wang, X.F., Liu, X.Zh., Wang, J., et al., *Russ. J. Coord. Chem.*, 2008, vol. 34, p. 134.
26. Zhang, L.Q., Fan, T.T., Wang, J., et al., *J. Coord. Chem.*, 2010, vol. 36, p. 389.
27. Wang, J., Wang, Y., Zhang, Zh.H., et al., *J. Struct. Chem.*, 2005, vol. 46, p. 895.
28. Ma, B.Q., Gao, S., and Jin, T.Zh., *Chem. J. Chin. Univ.*, 1999, vol. 20, p. 176.
29. Chen, Y., Ma, B.Q., Liu, Q.D., et al., *Inorg. Chem. Commun.*, 2000, vol. 3, p. 319.
30. Gao, J.Q., Wu, T., Wang, J., et al., *J. Coord. Chem.*, 2011, vol. 37, p. 817.
31. Bai, Y., Gao, J.Q., Wang, J., et al., *J. Coord. Chem.*, 2013, vol. 39, p. 147.
32. Gao, J.Q., Li, D., Wang, J., et al., *J. Coord. Chem.*, 2013, vol. 64, p. 2234.
33. Guggenberger, L.J. and Muetterties, E.L., *J. Am. Chem. Soc.*, 1976, vol. 98, p. 7221.